

Vibrational spectroscopic study of intensities and shifts of symmetric vibration modes of ozone diluted by cumene

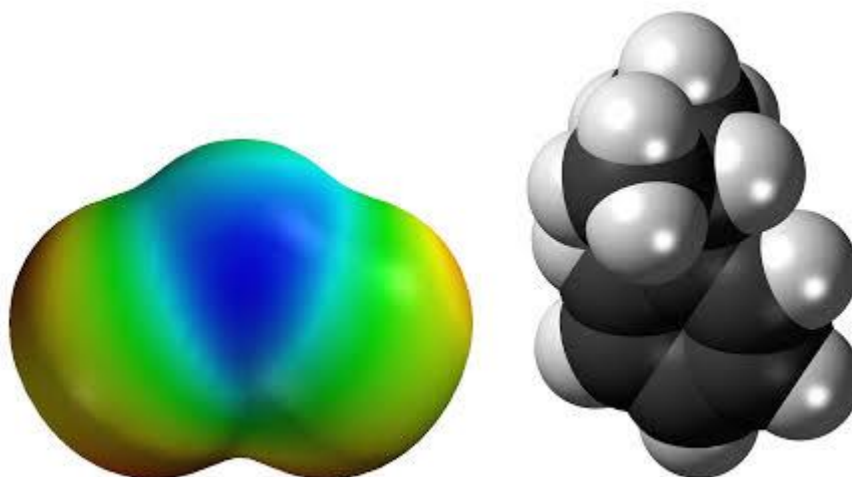
A. Heidari *, C. Brown

Faculty of Chemistry, California South University, 14731 Comet St. Irvine, CA 92604, USA

*Corresponding author E-mail: Scholar.Researcher.Scientist@gmail.com

Abstract

In the current research, ATR–FTIR and FT–Raman spectroscopies was used to investigate the effect of concentration on IR and Raman intensities and shifts of symmetric vibration modes of Ozone diluted by Cumene. The symmetric vibration mode of Ozone was observed at IR and Raman shifts of 850 and 975 cm^{-1} , respectively. By reducing the concentration of Ozone, its intensity also was reduced and the symmetric vibration mode of Cumene was observed at IR and Raman shifts of 1050 and 1185 cm^{-1} , respectively. The concentration has not influence on IR and Raman shifts of vibration modes. The experimental results were confirmed the linear dependency of IR and Raman intensities to the concentration of sample.



Ozone molecule (left illustration) and Cumene molecule (right illustration) (Santiago-López et al. 2010; Guevara-Guzmán et al. 2009; Pereyra-Muñoz et al. 2006; Foucaud et al. 2006; Elsayed 2001; van Hoof et al. 1997; Chrostowski et al. 1983; Boehme et al. 1992; Catalá et al. 2013; Balvers et al. 1992; Marker et al. 1986).

Keywords: Ozone Molecule; Cumene Molecule; Vibrational Spectroscopy; Attenuated Total Reflectance Fourier Transform Infrared Spectroscopy (ATR–FTIR); FT–Raman Spectroscopy; Vibration Modes.

1. Introduction

When laser light strikes to a sample, some part of incident light diffract. In the diffracted light, in addition to the frequency of incident light (Rayleigh diffraction), some rays observe at different frequencies which named as Raman diffraction. The frequency difference between incident and diffracted lights depends on vibration frequency of molecular bonds of materials. In ATR–FTIR and FT–Raman spectroscopies with recording the diffraction amount in each frequency, it is possible to find the molecular

structure of materials and hence, ATR–FTIR and FT–Raman spectroscopies can be used as finger print of materials (Santiago-López et al. 2010; Guevara-Guzmán et al. 2009; Pereyra-Muñoz et al. 2006; Foucaud et al. 2006; Elsayed 2001; van Hoof et al. 1997; Chrostowski et al. 1983; Boehme et al. 1992). Non destructivity and no need to sample preparation are the most important advantages of ATR–FTIR and FT–Raman spectroscopies (Catalá et al. 2013; Balvers et al. 1992; Marker et al. 1986; Isac-García et al. 2016; Anastas and Hammond 2016; Rodríguez-Reinoso and Silvestre-Albero 2016).

Ozone (O_3) is a linear, axisymmetric triatomic molecule with symmetry point of $D_{\infty h}$ (Ben Fredj et al. 2015; Gueneron et al. 2015). This molecule has four vibration modes that only one of them is symmetric and active in Raman. Its other vibration modes are active in IR (Babalou et al. 2015; Mattila et al. 2015). Cumene molecule (C_9H_{12}) with cyclic structure is belonged to symmetry group of D_{6h} . This molecule has 57 vibration modes that only 7 of them are active in IR and Raman and the remaining are active modes in ATR-FTIR and FT-Raman spectroscopies due to high symmetry of this molecule (Landaeta and Rodríguez-Lugo 2015; Ebnasajjad 2015).

In the current research, ATR-FTIR and FT-Raman spectroscopies was used in order to evaluate the effect of concentration on IR and Raman intensities and shifts of symmetric vibration modes of Ozone diluted by Cumene. The symmetrical vibration modes of Ozone and Cumene were observed at IR and Raman shifts of 850 and 975 cm^{-1} , respectively, and the effect of Ozone concentration on the intensity of these vibration modes was investigated. Further, the influence of sample concentration on the change of IR and Raman shifts of vibration modes was studied.

2. Materials, research method and experimental techniques

To perform this research, liquid O_3 and C_9H_{12} with 99% purity made by Sigma-Aldrich Co. were prepared. The liquid C_9H_{12} was

used as diluent for changing the O_3 concentration and its concentration was changed between 35% and 100% with incremental steps of 35%. ATR-FTIR and FT-Raman spectroscopies arrangement is shown in Figures (1) and (2). As Raman diffraction happens for only one of ten millions incident photons, sensitive and accurate optical apparatuses are needed in the arrangement. In this test, the second harmonic continuous laser Nd:YAG with power of 75 mW is used. A passing filter was inserted after laser to reduce spectroscopic width of incident ray. Then, laser ray was focused on quartz cell containing the sample using L_1 lens ($f=60$ mm) and the diffracted light from it was collected at 90 degrees angle by L_2 lens ($f=35$ mm) before entering to notch filter. As Raman diffraction intensity is very weaker than Rayleigh diffraction, notch filter was used to remove elastic Rayleigh diffraction. The diffracted light from L_2 lens ($f=35$ mm) was focused on optical fiber of spectroscope and was detected by CCD after separation. Spectra of samples were recorded in the spectral range of 0–4000 cm^{-1} and with separation accuracy of 17.4 cm^{-1} .

3. Results and discussion

ATR-FTIR and FT-Raman spectra of liquid O_3 for six different concentrations are shown in Figures (3) and (4). OriginPro 9.1 software was used to draw the spectra.

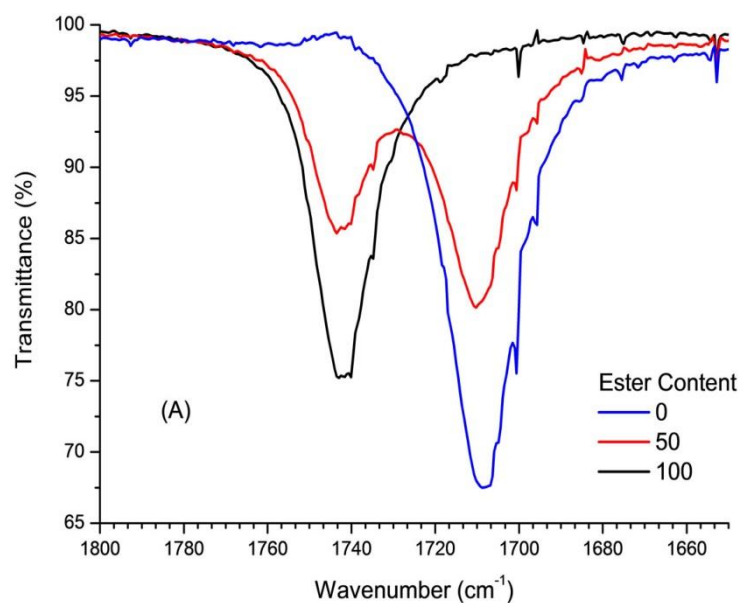


Fig. 1: Schematic View of ATR-FTIR Spectroscopy Arrangement.

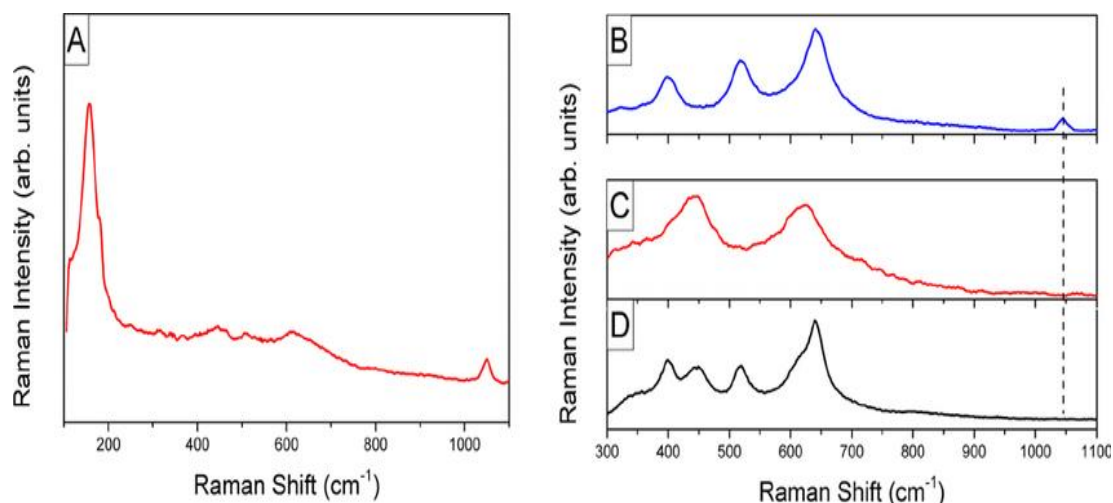


Fig. 2: Schematic View of FT-Raman Spectroscopy Arrangement.

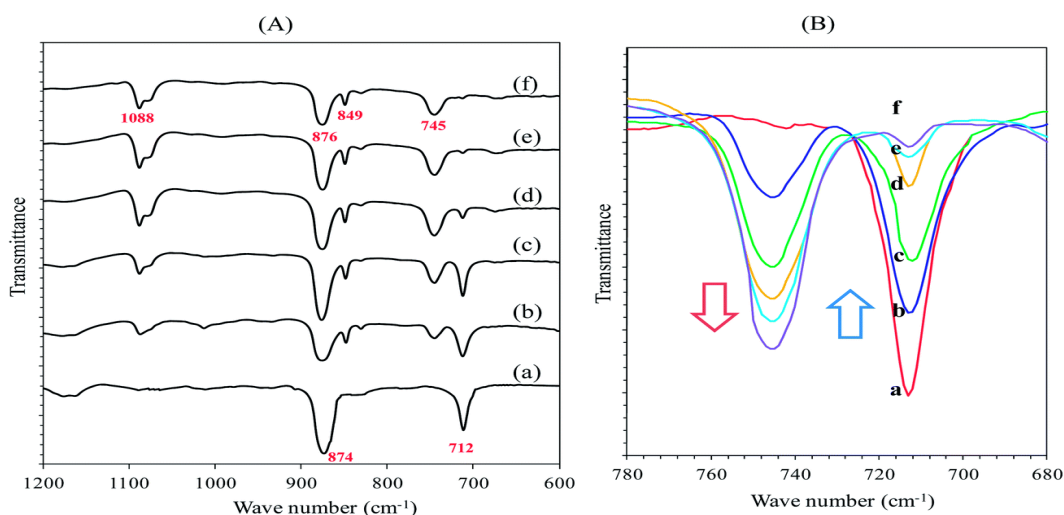


Fig. 3: ATR-FTIR Spectrum at Various Concentrations of O_3 .

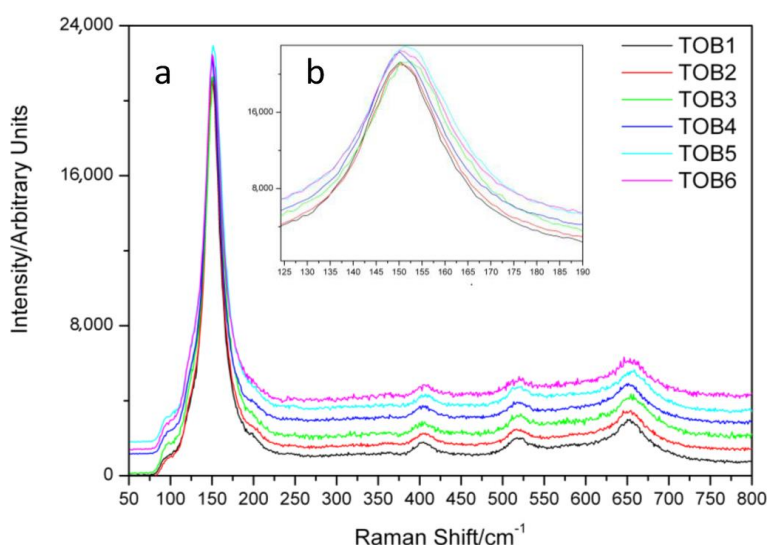


Fig. 4: FT-Raman Spectrum at Various Concentrations of O_3 .

According to these Figures, symmetric vibration mode of O_3 is observed at IR and Raman shifts of 850 and 975 cm^{-1} respectively and its intensities is increased with increase in concentration of O_3 . At the other hand, by reducing the concentration of C_9H_{12} at the solution, the intensity of peak point related to Raman shift of symmetric vibration mode of the liquid is reduced at wavenumber of 1050 and 1185 cm^{-1} , respectively.

As none of studied samples have no active IR and Raman modes in wavenumber ranges from 200–1200 cm^{-1} , the observed peaks in this region are not related to the studied samples. Regarding the fact that the cell is made from quartz and the strongest IR and Raman vibration modes are in this range, it can be concluded that the observed peaks are related to quartz. It should be noted that the intensity of these peaks are increased by increasing the concentration of O_3 . The wide-band incident laser leads to widening the vibration mode peak of 850 and 975 cm^{-1} respectively for O_3 and by placing the vibration modes of quartz on the flange of the above wide-band vibration mode in various concentrations, the intensity of these modes also increase by increasing the concentration of O_3 . In the wavenumber ranges from 500–2500 cm^{-1} , the irregularities in the spectrum are related to the noise of spectroscopy which superposition of spectrum of various samples with changing the concentration approves this issue. Although Cumene has some active IR and Raman vibration modes in this region, the peaks have not been observed due to the very small diffraction cross section of these modes compared to the detected vibration modes.

In the spectra shown in Figures (3) and (4) for symmetric vibration modes of O_3 at 850 and 975 cm^{-1} respectively and also C_9H_{12}

at 1050 and 1185 cm^{-1} respectively, there is not any considerable shift for wavenumber by changing the concentration of samples. This is in good agreement with the results obtained by other researchers (Santiago-López et al. 2010; Guevara-Guzmán et al. 2009; Pereyra-Muñoz et al. 2006; Foucaud et al. 2006; Elsayed 2001; van Hoof et al. 1997; Chrostowski et al. 1983; Boehme et al. 1992; Catalá et al. 2013; Balvers et al. 1992; Marker et al. 1986; Isac-García et al. 2016; Anastas and Hammond 2016; Rodríguez-Reinoso and Silvestre-Albero 2016; Ben Fredj et al. 2015; Gueneron et al. 2015; Babalou et al. 2015; Mattila et al. 2015; Landaeta and Rodríguez-Lugo 2015; Ebnesajjad 2015).

Therefore, the IR and Raman intensities for each vibration mode are a function of cross section of the mode with power two. The Raman diffraction cross sectional area for vibration mode of O_3 at 975 cm^{-1} is larger than the Raman diffraction cross sectional area for vibration mode of C_9H_{12} at 1185 cm^{-1} and this is the reason for larger intensity of vibration mode for O_3 than C_9H_{12} in Figures (3) and (4). If the Raman diffraction cross sectional area and the intensity of incident laser are constant, the intensities of IR and Raman signals is directly related to the concentration of sample. The 3D-variations of IR and Raman intensities of vibration modes for these two liquids as a function of concentration are shown in Figures (5) and (6). According to these Figures, the linear dependency of Raman intensity to concentration can be seen for both materials.

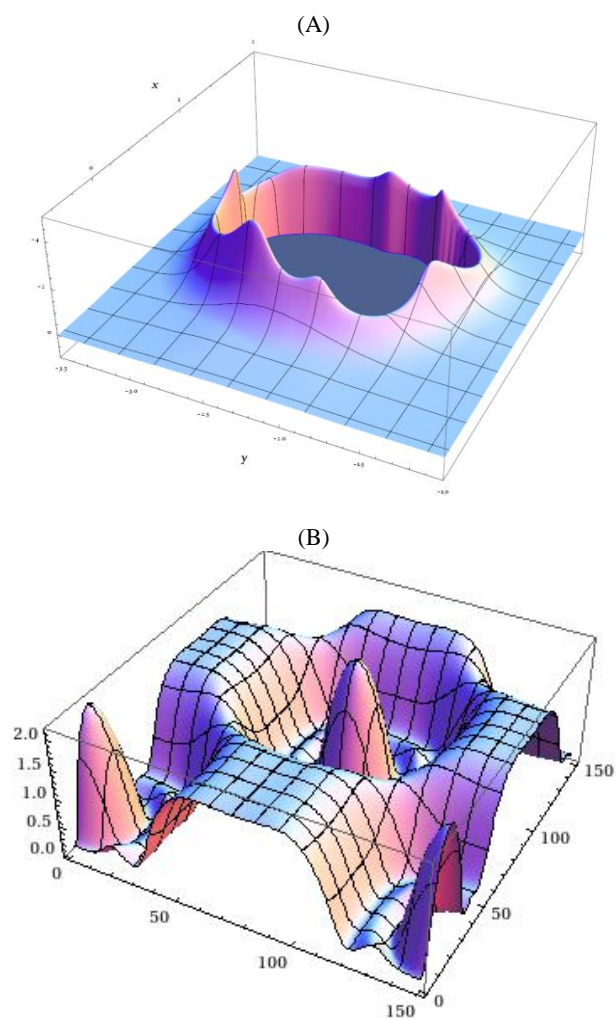
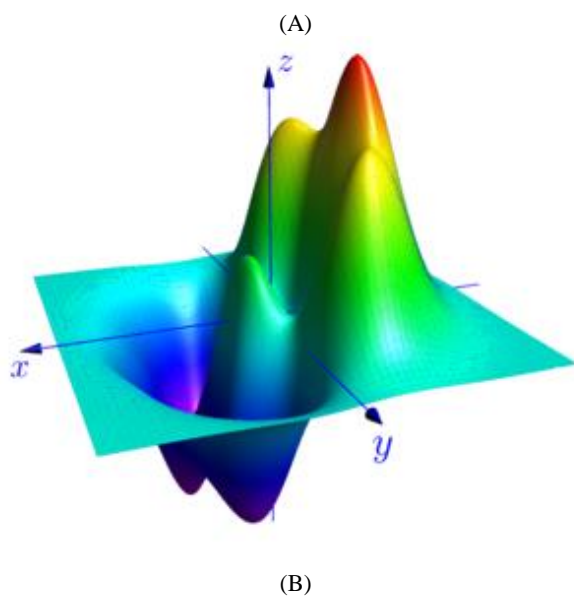


Fig. 5: 3D-IR Intensities Elated To Vibration Modes of (A) O₃ at 850 Cm⁻¹ and (B) C₉H₁₂ at 1050 Cm⁻¹ as a Function of Concentration.



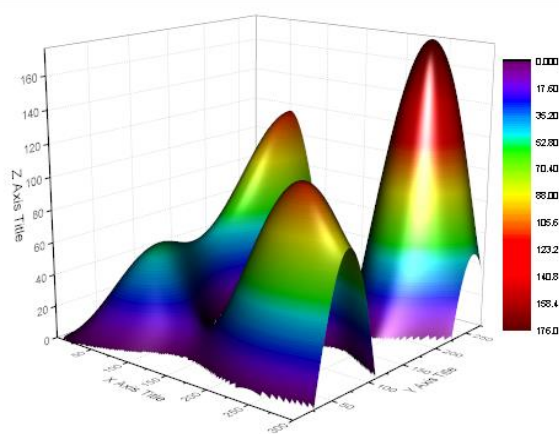


Fig. 6: 3D-Raman Intensities Elated to Vibration Modes of (A) O_3 at 975 cm^{-1} and (B) C_9H_{12} at 1185 cm^{-1} as A Function of Concentration.

4. Conclusion

ATR-FTIR and FT-Raman spectroscopies are an applicable method for investigating the molecular structures and vibration modes of molecules. In the current research, IR and Raman intensities of symmetric vibration modes for O_3 at 850 and 975 cm^{-1} respectively were increased by increasing the concentration of O_3 and the IR and Raman intensities of symmetric vibration modes for C_9H_{12} at 1050 and 1185 cm^{-1} respectively were decreased by increasing the concentration of C_9H_{12} . If the Raman cross sectional area and the intensity of incident laser are constant, the intensities of IR and Raman signals is directly related to the concentration of sample. The linear dependency to concentration was observed for both samples. At the other hand, concentration has no effect on IR and Raman shifts of the considered vibration modes.

References

- [1] D. Santiago-López, J.A. Bautista-Martínez, C.I. Reyes-Hernandez, M. Aguilar-Martínez, S. Rivas-Arancibia, Oxidative stress, progressive damage in the substantia nigra and plasma dopamine oxidation, in rats chronically exposed to ozone, *Toxicology Letters*, Volume 197, Issue 3, 1 September 2010, Pages 193-200. <http://dx.doi.org/10.1016/j.toxlet.2010.05.020>.
- [2] R. Guevara-Guzmán, V. Arriaga, K.M. Kendrick, C. Bernal, X. Vega, O.F. Mercado-Gómez, S. Rivas-Arancibia, Estradiol prevents ozone-induced increases in brain lipid peroxidation and impaired social recognition memory in female rats, *Neuroscience*, Volume 159, Issue 3, 31 March 2009, Pages 940-950. <http://dx.doi.org/10.1016/j.neuroscience.2009.01.047>.
- [3] Naira Pereyra-Muñoz, Concepción Rugerio-Vargas, Mariana Angoa-Pérez, Gabino Borronio-Pérez, Selva Rivas-Arancibia, Oxidative damage in substantia nigra and striatum of rats chronically exposed to ozone, *Journal of Chemical Neuroanatomy*, Volume 31, Issue 2, February 2006, Pages 114-123.
- [4] L. Foucaud, A. Bennisroune, D. Klestadt, P. Laval-Gilly, J. Falla, Oxidative stress induction by short time exposure to ozone on THP-1 cells, *Toxicology in Vitro*, Volume 20, Issue 1, February 2006, Pages 101-108. <http://dx.doi.org/10.1016/j.tiv.2005.06.007>.
- [5] Nabil M Elsayed, Diet restriction modulates lung response and survivability of rats exposed to ozone, *Toxicology*, Volume 159, Issue 3, 28 February 2001, Pages 171-182.
- [6] H.J.M. van Hoof, H.-P. Voss, K. Kramer, A.J.F. Boere, J.A.M.A. Dormans, L. van Bree, A. Bast, Changes in neuroreceptor function of tracheal smooth muscle following acute ozone exposure of guinea pigs, *Toxicology*, Volume 120, Issue 3, 11 July 1997, Pages 159-169. [http://dx.doi.org/10.1016/S0300-483X\(96\)03603-7](http://dx.doi.org/10.1016/S0300-483X(96)03603-7).
- [7] Paul C. Chrostowski, Andrea M. Dietrich, Irwin H. Suffet, Ozone and oxygen induced oxidative coupling of aqueous phenolics, *Water Research*, Volume 17, Issue 11, 1983, Pages 1627-1633.
- [8] D.S. Boehme, J.A. Hotchkiss, R.F. Henderson, Glutathione and GSH-dependent enzymes in bronchoalveolar lavage fluid cells in response to ozone, *Experimental and Molecular Pathology*, Volume 56, Issue 1, February 1992, Pages 37-48. [http://dx.doi.org/10.1016/0014-4800\(92\)90021-3](http://dx.doi.org/10.1016/0014-4800(92)90021-3).
- [9] M. Catalá, F. Gasulla, A.E. Pradas del Real, F. García-Breijo, J. Reig-Armiñana, E. Barreno, The organic air pollutant cumene hydroperoxide interferes with NO antioxidant role in rehydrating lichen, *Environmental Pollution*, Volume 179, August 2013, Pages 277-284. <http://dx.doi.org/10.1016/j.envpol.2013.04.015>.
- [10] Walter G. Balvers, Marelle G. Boersma, Cees Veeger, Ivonne M.C.M. Rietjens, Differential cumene hydroperoxide sensitivity of cytochrome P-450 enzymes IA1 and IIB1 determined by their way of membrane incorporation, *Biochimica et Biophysica Acta (BBA) - General Subjects*, Volume 1117, Issue 2, 15 September 1992, Pages 179-187.
- [11] Elizabeth K. Marker, Arun P. Kulkarni, Cumene hydroperoxide-supported denitrification of 2-nitropropane in uninduced mouse liver microsomes, *International Journal of Biochemistry*, Volume 18, Issue 7, 1986, Pages 595-601.
- [12] Joaquín Isac-García, José A. Dobado, Francisco G. Calvo-Flores and Henar Martínez-García, Chapter 1 - Laboratory Safety, In *Experimental Organic Chemistry*, Academic Press, 2016, Pages 1-28. <http://dx.doi.org/10.1016/B978-0-12-803893-2.50001-2>.
- [13] Paul T. Anastas and David G. Hammond, Chapter 4 - Case Studies—Green Chemistry in Practice, In *Inherent Safety at Chemical Sites*, Elsevier, 2016, Pages 23-118. <http://dx.doi.org/10.1016/B978-0-12-804190-1.00004-5>.
- [14] F. Rodriguez-Reinoso and J. Silvestre-Albero, Activated Carbon and Adsorption, In *Reference Module in Materials Science and Materials Engineering*, Elsevier, 2016, Current as of 28 October 2015.
- [15] S. Ben Fredj, J. Nobbs, C. Tizaoui, L. Monser, Removal of estrone (E1), 17β -estradiol (E2), and 17α -ethinylestradiol (EE2) from wastewater by liquid-liquid extraction, *Chemical Engineering Journal*, Volume 262, 15 February 2015, Pages 417-426. <http://dx.doi.org/10.1016/j.cej.2014.10.007>.
- [16] Mylene Gueneron, Mathew H. Erickson, Graham S. VanderSchelden, Bertram T. Jobson, PTR-MS fragmentation patterns of gasoline hydrocarbons, *International Journal of Mass Spectrometry*, Volume 379, 15 March 2015, Pages 97-109. <http://dx.doi.org/10.1016/j.ijms.2015.01.001>.
- [17] A.A. Babalou, N. Rafia and K. Ghasemzadeh, 3 - Integrated systems involving pervaporation and applications, In *Woodhead Publishing Series in Energy*, edited by Angelo Basile and Alberto FigoliMohamed Khayet, Woodhead Publishing, Oxford, 2015, Pages 65-86. <http://dx.doi.org/10.1016/b978-1-78242-246-4.00003-9>.
- [18] Heta Mattila, Sergey Khorobrykh, Vesa Havurinne, Esa Tyystjärvi, Reactive oxygen species: Reactions and detection from photosynthetic tissues, *Journal of Photochemistry and Photobiology B: Biology*, Volume 152, Part B, November 2015, Pages 176-214.
- [19] Vanessa R. Landaeta, Rafael E. Rodríguez-Lugo, Catalytic oxygenation of organic substrates: Toward greener ways for incorporating oxygen, *Inorganica Chimica Acta*, Volume 431, 24 May 2015, Pages 21-47.
- [20] Sina Ebnesajjad, 8 - Polymerization and Finishing Melt-Processible Fluoropolymers, In *Fluoroplastics (Second Edition)*, William Andrew Publishing, Oxford, 2015, Pages 102-215. <http://dx.doi.org/10.1016/B978-1-4557-3197-8.00008-0>.